Physics – Uspekhi **66** (9) 951 – 960 (2023)

METHODOLOGICAL NOTES PACS numbers: 43.30.Cq, 43.30.Dr

Isolation of the field component formed by a given beam of rays at the aperture of a receiving antenna in an inhomogeneous environment

A L Virovlyansky

DOI: https://doi.org/10.3367/UFNe.2022.08.039229

Contents

Abstract. A generalization of the classical procedure for forming a receiving antenna beam in a homogeneous space to the case of an inhomogeneous medium is discussed. In free space, this procedure isolates the component of the registered field, which represents the contribution of a beam of parallel rays. In an inhomogeneous medium, the procedure should isolate the contribution of a beam of rays, which, as a rule, are not parallel. The generalization is carried out on the basis of the transition from the traditional representation of the registered field in the form of a superposition of plane waves to the coherent state expansion of the field borrowed from quantum mechanics. The general approach is illustrated using the example of the lobe formation of a vertical receiving antenna in an underwater acoustic waveguide.

Keywords: antenna, beamforming, beam of rays, coherent state, acoustic waveguide

1. Introduction

A conventional beamforming method for a receiving antenna assumes that the registered field component is that part of a plane wave corresponding to the arrival of a beam of *parallel* rays [1]. This field component has a spatial frequency $\kappa_\alpha = k \sin\alpha$ on the antenna aperture, where k is the wavenumber and α is the angle of beam incidence. The beamforming takes place through spatial filtering of the field received in the band $\kappa_\alpha \pm 2\pi/L$, where L is the antenna size. The filter 'passes' signals that come from a relevant source and 'cuts out' signals from other directions. This method is oriented toward applications in an environment which can be considered homogeneous, at least approximately.

In this paper, we consider a generalization of this method to the case of an inhomogeneous environment, where multipath propagation takes place and the field on the antenna is formed by several ray beams. A principal point is that the rays making an individual beam are as a rule *not parallel*.

As an example of such an environment, we consider below an underwater waveguide in the deep sea. It is assumed that a field emitted by a point source is received by a vertical antenna.

The key idea underlying our approach is formulated in Ref. [2] (see also [3]). It consists in moving from the traditional expansion of the field at the antenna in plane waves to the expansion in coherent states borrowed from quantum mechanics [4, 5]. This expansion establishes a link between the ray and wave field representations and allows one to find the distribution of complex field amplitude in the phase plane angle χ–depth z. This plane is an example of a phase plane used in Hamilton's formulation of classical mechanics and geometrical optics [6–8]. An arrival of a ray to the observation distance is depicted by a point in the phase plane.

A coherent state is associated with every point of the phase plane (χ, z). The projection of the received field on this state singles out the contributions from waves arriving at the depth horizons close to z under angles close to χ. The use of the coherent state expansion allows creating a spatial filter which isolates a field component that corresponds to the contribution of a given ray beam. In the vicinity of point z on the antenna aperture, the grazing angles of waves forming the component are close to the grazing angle χ of the ray from the selected beam that arrives at this point. This filter defines the beamforming tuned to the beam registration. In the case of parallel rays, a conventional lobe of directivity pattern in a free space is formed.

A L Virovlyansky
Federal Research Center A V Gaponov-Grekhov Institute of Applied Physics, Russian Academy of Sciences, ul. Ul'yanova 46, 603950 Nizhny Novgorod, Russian Federation
E-mail: viro@ipfran.ru

Received 20 May 2022, revised 6 August 2022
Uspekhi Fizicheskikh Nauk **193** (9) 1010 – 1020 (2023)
Translated by S D Danilov

The material in this study is arranged as follows. Section 2 describes a model of an underwater waveguide used to illustrate and test the described method. The main relationships defining the coherent state expansion are given in Section 3. Section 4 presents the results of numerical calculations which characterize the sensitivity of field intensity distribution in the phase plane to the sound speed fluctuations in the waveguide. The procedure of beamforming in an inhomogeneous environment is presented in Section 5. In Section 6, an estimate of 'noise' that 'percolates' through a filter tuned to extract a given beam is carried out. Section 7 shows that the method to isolate beam contributions, discussed in this paper, can also be used to solve the problem of sound source localization (estimate of coordinates) in a waveguide. Sections 3–7 deal with a pointwise tonal source. Section 8 briefly considers the application of the discussed procedure to a field excited by a pulsed source. Section 9 summarizes the work.

2. Environment model

To illustrate general statements, we use an idealized model of the inhomogeneous environment, which is taken to be a sound waveguide in the deep sea. To avoid discussion of secondary details, we limit ourselves to a two-dimensional case with the sound speed field $c(r, z)$, where r is the horizontal distance and z is the depth. Let $c(r, z) = c_b(z) + \delta c(r, z)$, where $c_b(z)$ is the unperturbed profile (Fig. 1a) and $\delta c(r, z)$ is a random function which describes weak fluctuations of the sound speed. The z-axis is directed vertically downward, and the water surface is located at $z = 0$.

The plane-layered waveguide ($\delta c = 0$) is considered further as an available (approximate) model of a real fluctuating environment. We assume that the flat bottom at a 3-km depth is highly absorbing. As a result, the sound field on the horizon $z_s = 0.7$ km is created by waves trapped in the refraction waveguide and propagating without bottom reflections. These waves are formed by rays emanating from the source at launch angles lying in the interval $\pm\chi_{\max}$, where $\chi_{\max} = 12.5°$.

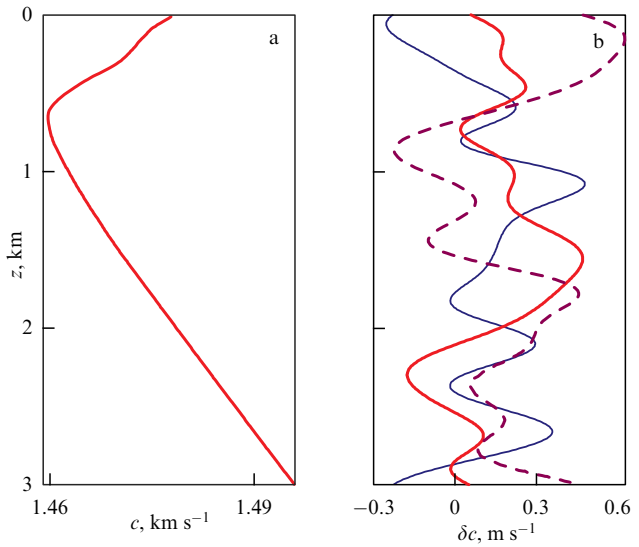

Figure 1. (a) Unperturbed sound speed profile $c_b(z)$. (b) Examples of realizations of random perturbation δc in vertical waveguide section.

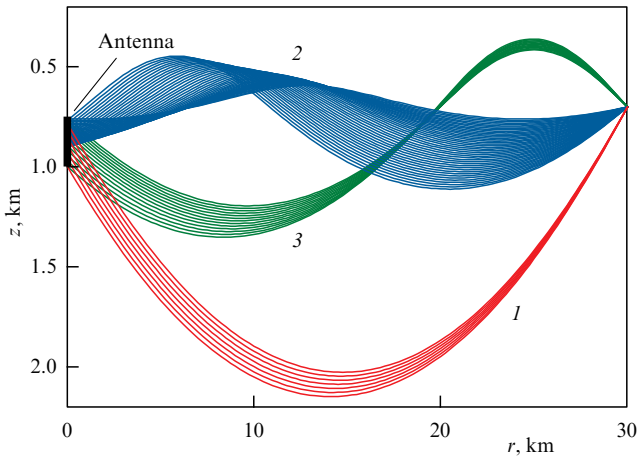

Figure 2. Trajectories of rays leaving a point source and crossing the aperture of a receiving antenna (coordinates of antenna endpoints are given in the text). These rays form three beams, each labelled by their numbers.

Fluctuations in the sound speed field will be modeled by the function $\delta c(r, z)$ with zero mean $\langle \delta c \rangle = 0$ and the correlation function

$$\langle \delta c(r, z)\, \delta c(r', z') \rangle = (\delta c_{\text{rms}})^2 \exp\left(-\frac{\pi (r - r')^2}{l_r^2} - \frac{\pi (z - z')^2}{l_z^2} \right),$$

where $\delta c_{\text{rms}} = 0.25$ m s^{-1}, $l_r = 5$ km, and $l_z = 0.5$ km. Here and below, the notation $\langle \ldots \rangle$ implies averaging over an ensemble of random realizations. This simple model differs from more realistic ones used in underwater acoustics to describe sound speed fluctuations in the deep sea [9, 10]. However, Ref. [11] shows that it is well suited for the analysis of sound field components formed by the narrow ray beams we are interested in. Figure 1b plots several realizations of δc in vertical waveguide sections.

The refraction index is $n(r, z) = c_0/c(r, z)$, where c_0 is the reference speed of sound. In underwater acoustics, the scatter in values of $c(r, z)$ is commonly small and c_0 can be assigned a value that satisfies the condition $|c(r, z) - c_0| \ll c_0$. In our example, we take $c_0 = 1.47$ km s^{-1}. In this case, $n(r, z)$ is close to unity.

Further, we shall consider fields at the aperture of a vertical receiving antenna with a length of 250 m, located on the line $r = 0$ and covering the depth range $z_1 < z < z_2$, where $z_1 = 0.75$ km, and $z_2 = 1$ km. Figure 2 shows ray trajectories in an unperturbed waveguide which leave a point source S located at distance $r_s = 30$ km and depth $z_s = 0.7$ km and reach the antenna. The rays form three beams, and the subject of our analysis is their isolation. Note that the antenna intersects a caustic, which is touched by rays forming beam *2*.

Below, all calculations of fields excited by a point tonal source are carried out for the carrier frequency $f = 500$ Hz. In modeling the propagation of pulsed signals, this frequency is the central one. Sound fields are computed using the method of the wide-angle parabolic equation [12].

3. Coherent state expansion of sound field

To describe ray trajectories, we will use Hamilton's formalism [8, 13] in the framework of which the trajectory at each point of distance r is given by vertical coordinate (depth) z and

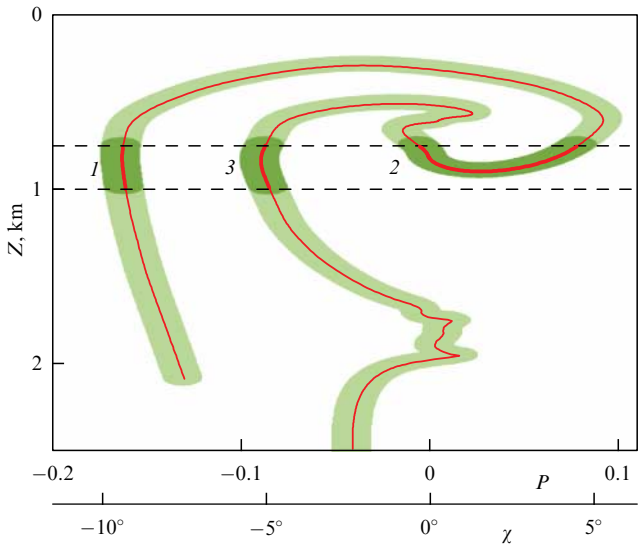

Figure 3. Ray line (thin line) and fuzzy ray line (domain shaded in light green) at a distance of 30 km from the source. Dashed lines mark the depths of antenna endpoints. Solid intervals of the ray line correspond to the arrival of rays which form the three beams shown in Fig. 2. Dark green color highlights the fuzzy segments which correspond to individual beams. Each segment is labelled by the number of the respective beam.

momentum $p = n(r, z)\sin\chi$, where χ is the ray grazing angle. Trajectories are governed by Hamilton's equations $\mathrm{d}z/\mathrm{d}r = \partial H/\partial p$ and $\mathrm{d}p/\mathrm{d}r = -\partial H/\partial z$ with the Hamiltonian $H = -[n^2(r,z) - p^2]^{1/2}$. If the field is excited at the point (r_s, z_s), all the rays emanate from one and the same depth z_s but with different initial momenta p_s. At the distance of observation, the arrival of each ray is plotted by a point in the phase plane the momentum P–coordinate Z. The union of such points forms a curve called a geometric ray line or simply a ray line. In mechanics, it is referred to as a Lagrangian manifold [14]. Since in our case n is close to one and propagation angles χ are small, the phase plane can be interpreted as the plane angle–coordinate.

The thin solid line in Fig. 3 depicts a ray line describing the arrivals of rays at the distance $r = 0$ from the source S (see Fig. 2). Straight dashed lines indicate horizons that correspond to antenna endpoints. They 'cut' segments of the ray line that correspond to arrivals of the three beams shown in Fig. 2. These segments are shown by bold line intervals, each labelled by the number of the respective beam. Note that on the segment that corresponds to beam *2* there is a point where the tangent to the ray line is horizontal. This point depicts the arrival of a ray that touches a caustic at the observational distance [14]. In Fig. 3, as well as in Figs 4 and 5 further, a second axis is drawn under the abscissas showing ray arrival angles χ, which corresponds to momenta P.

To clarify the relation between ray trajectories and the wave field for a finite wavelength, we turn to the field representation through the coherent state expansion which is borrowed from quantum mechanics [4, 5, 15]. We will consider a field excited by a point tonal source with angular frequency ω.

The coherent state, or the state with minimum uncertainty, associated with point $\mu = (P, Z)$ in the phase plane, is given by the function

$$Y_\mu(z) = \frac{1}{\sqrt{\Delta_z}} \exp\left[\mathrm{i}kP(z - Z) - \frac{\pi(z - Z)^2}{2\Delta_z^2}\right], \qquad (1)$$

where Δ_z is the spatial scale of the state and $k = \omega/c_0$ is the reference wavenumber. In quantum mechanics, (1) describes a state with the minimum product of the variances of coordinate and momentum [16], while in acoustics it can be interpreted as the vertical section of a beam with width Δ_z propagating under grazing angle $\chi = \arctan P$. Although the coherent states are not orthogonal, they form a complete set of functions. An arbitrary function $u(z)$ can be expanded as [4]

$$u(z) = \lambda^{-1} \int \mathrm{d}\mu\, a_\mu Y_\mu(z), \qquad (2)$$

where the integration is performed over the entire phase plane, $\lambda = 2\pi/k$ is the wavelength, $\mathrm{d}\mu = \mathrm{d}P\,\mathrm{d}Z$, and

$$a_\mu = \int_{-\infty}^{\infty} \mathrm{d}z\, u(z)\, Y_\mu^*(z). \qquad (3)$$

Let us mention a convenient formula which follows from (2) and (3),

$$\int \mathrm{d}\mu\, |a_\mu|^2 = \lambda^{-1} \int_{-\infty}^{\infty} \mathrm{d}z\, |u(z)|^2, \qquad (4)$$

and which we will need further.

A scalar product of coherent states associated with points $\mu_1 = (P_1, Z_1)$ and $\mu_2 = (P_2, Z_2)$ is

$$\left| \int \mathrm{d}z\, Y_{\mu_1}(z) Y_{\mu_2}^*(z) \right| = \exp\left(-\frac{\pi}{2}\, d(\mu_1, \mu_2)\right), \qquad (5)$$

where

$$d(\mu_1, \mu_2) = \frac{(P_2 - P_1)^2}{\Delta_p^2} + \frac{(Z_2 - Z_1)^2}{\Delta_z^2}, \qquad (6)$$

and $\Delta_p = \lambda/(2\Delta_z)$. The function $d(\mu_1, \mu_2)$ can be treated as a dimensionless distance between phase plane points μ_1 and μ_2. The coherent states associated with these points will be considered close for $d < 1$ and distant if $d > 1$. The distance from an arbitrary point of the plane to the ray line (or its segment) will be defined as that to the nearest point of this line (segment).

The main contribution to the sound field comes from coherent states associated with points μ separated from the ray line by the distance $d < 1$. This region is referred to as a fuzzy ray line. Its area is determined by the choice of the coherent state scales Δ_z and Δ_p. Since they are linked by the uncertainty relation

$$\Delta_z \Delta_p = \frac{\lambda}{2}, \qquad (7)$$

we in fact can choose only one of them. Reference [3] discusses the question of the selection of Δ_z that would minimize the area of the fuzzy ray line. Clearly, if $\Delta_z \to 0$ and $\Delta_z \to \infty$, the area will increase unboundedly. A minimum is reached for some finite Δ_z which is governed by the shape of the ray line. In Ref. [3], it is shown that this scale is proportional to $\lambda^{1/2}$. In our case, the minimum of area is reached for $\Delta_z = 0.09$ km. The respective fuzzy ray line is shaded in light green in Fig. 3.

The beam contribution to the total wave field is formed by the coherent states associated with the phase plane points μ at the distance $d < 1$ from the segment of the ray line represent-

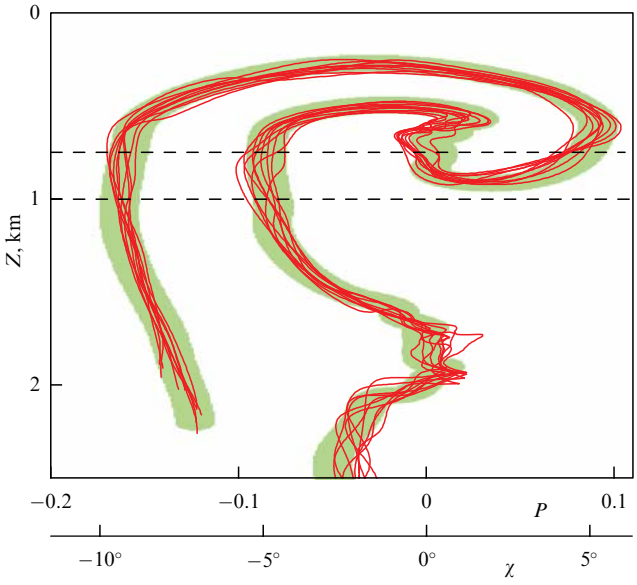

Figure 4. Ray lines computed for 10 realizations of random perturbation $\delta c(r, z)$. Source is at a distance of 30 km. Light green color shows the same fuzzy ray line as in Fig. 3. Dashed lines indicate antenna endpoints.

ing the beam. These points form the regions of the fuzzy ray line which will be referred to as fuzzy segments. In Fig. 3, the fuzzy segments that correspond to our three beams are shaded in dark green.

4. Field intensity distribution in the phase plane

In this section, we present the results of numerical simulations demonstrating the effect of perturbations δc on the ray structure and the distribution of field intensity in the waveguide model considered here.

Figure 4 shows ray lines computed by numerically solving Hamilton's equations (ray equations) for 10 realizations of random perturbation $\delta c(r, z)$. Each line depicts arrivals at the distance of observation of the rays leaving the source under grazing angles at the interval of $\pm 12°$. As can be seen, these lines are confined almost everywhere to the light green domain (the same as in Fig. 3), which is the fuzzy ray line of the unperturbed waveguide. This means that the distribution of coherent state intensity $|a_\mu|^2$ in the presence of random perturbation should be localized in approximately the same phase space domain (fuzzy ray line) as in the unperturbed waveguide. Figure 5 shows that this is indeed the case. It shows the distributions of coherent state intensities $|a_\mu|^2$ in the unperturbed waveguide (a) and in the presence of one realization of perturbation δc (b). The solid white line shows the boundaries of the fuzzy ray line in the unperturbed waveguide which is shown in Figs 3 and 4.

Figure 6 shows the dependences of sound field intensity $|u(z)|^2$ on depth in an unperturbed waveguide (red line) and in the presence of random perturbation δc (blue line). Comparing Figs 5 and 6, we see that, even though perturbation δc cardinally modifies the depth dependence of field intensity on the antenna, it only weakly influences the distribution of field intensity in the phase plane. This difference is explained by the fact that there are no multipath effects in the phase plane [3]. Let us look at this in more detail.

The total field $u(z)$ is a superposition of components $u_n(z)$, $n = 1, 2, 3$, each formed by one of the ray beams shown in

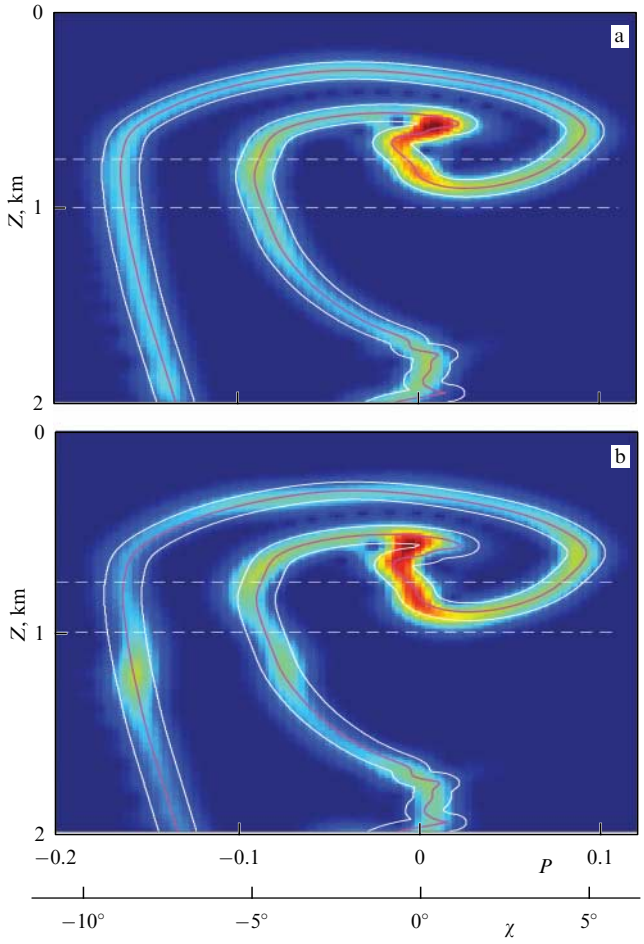

Figure 5. Distributions of coherent state intensity $|a_\mu|^2$ in an unperturbed waveguide (a) and in the presence of perturbations δc (b). Solid violet curve and white lines (the same in panels a and b) depict, respectively, the geometrical ray line and the boundaries of the fuzzy ray line in the unperturbed waveguide. Dashed lines show antenna endpoints.

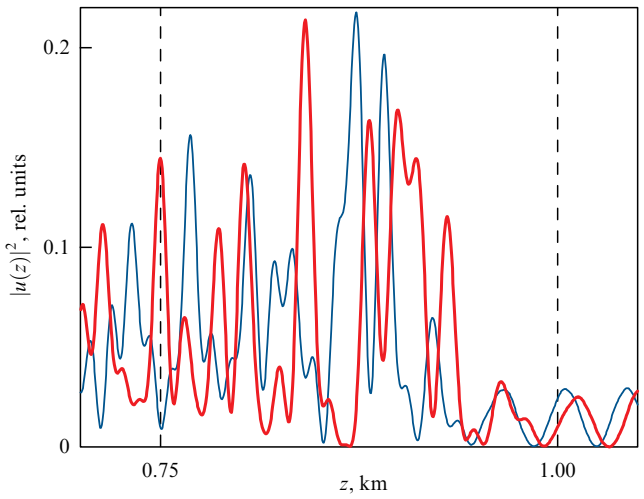

Figure 6. Depth dependence of field intensity in an unperturbed waveguide (red line) and in the presence of one realization of perturbation δc (blue line). Vertical lines show antenna endpoints.

Fig. 2. The width of each beam does not exceed the vertical scale of perturbation δc. For this reason, the rays of the nth beam cross approximately the same inhomogeneities, and

their phases acquire approximately the same increments ϕ_n. Since the inhomogeneities crossed by different beams are uncorrelated, the increments ϕ_n that correspond to different n are statistically independent. Despite δc being small, the values of ϕ_n can exceed π and the superposition of the component $u_n(z)$ in the presence and absence of fluctuations can be cardinally different. Namely this is seen in Fig. 6.

In agreement with the discussion above, the effect of fluctuations on the component $u_n(z)$ can be roughly accounted for by multiplying it by $\exp(i\phi_n)$. According to (3), the influence of fluctuations on the amplitudes of coherent states a_μ associated with the points of the fuzzy segment σ_n is approximately accounted for by the multiplication of all such a_μ by the same phase multiplier, which does not change $|a_\mu|^2$. This explains the stability of the distribution of coherent state intensity $|a_\mu|^2$ against perturbation δc, seen in Fig. 5.

The circumstance that ray lines in Fig. 4 almost always stay within the confines of the fuzzy ray line of the unperturbed waveguide is the consequence of δc being weak in the case considered. An increase in δc will cause a stronger deviation of the ray line from its position in the unperturbed waveguide. In this case, the distribution of intensity $|a_\mu|^2$ will be localized in a wider phase plane region.

5. Isolation of the field component formed by a given ray beam

We return to Fig. 5 and remark that in both unperturbed and perturbed waveguides the intensity is localized inside of fuzzy segments σ_n, $n = 1, 2, 3$, computed for $\delta c = 0$, which are shown in Fig. 3. This means that, in the presence of perturbation, field component $u_n(z)$, representing the contribution of the nth beam, is formed by the superposition of practically the same coherent states as for $\delta c = 0$. It should, however, be stressed that the complex amplitudes of these states a_μ depend on perturbations δc, and therefore the components $u_n(z)$ are random functions.

It is assumed that the antenna length L is substantially larger than the scale Δ_z. In this case, the coherent state amplitudes a_μ, associated with the points in the domain σ_n, can be found by formula (3), where integration is carried out over the antenna aperture. The field component $u_n(z)$ is given by the superposition of such states [2]:

$$u_n(z) = \lambda^{-1} \int_{\sigma_n} \mathrm{d}\mu \, a_\mu Y_\mu(z) \,. \tag{8}$$

Using (3), for an antenna covering the depth range $z_1 < z < z_2$, expression (8) can be rewritten as

$$u_n(z) = \int_{z_1}^{z_2} \Pi_n(z, z') \, u(z') \, \mathrm{d}z' \,, \tag{9}$$

where

$$\Pi_n(z, z') = \lambda^{-1} \int_{\sigma_n} \mathrm{d}\mu \; Y_\mu(z) \; Y_\mu^*(z') \,. \tag{10}$$

Thus, the isolation of the beam contribution in the total field is realized with the help of linear spatial filtering. The filter parameters are defined by the fuzzy segment, which is computed for the *unperturbed* waveguide. By selecting σ_n, the filter is 'tuned' to the desired beam.

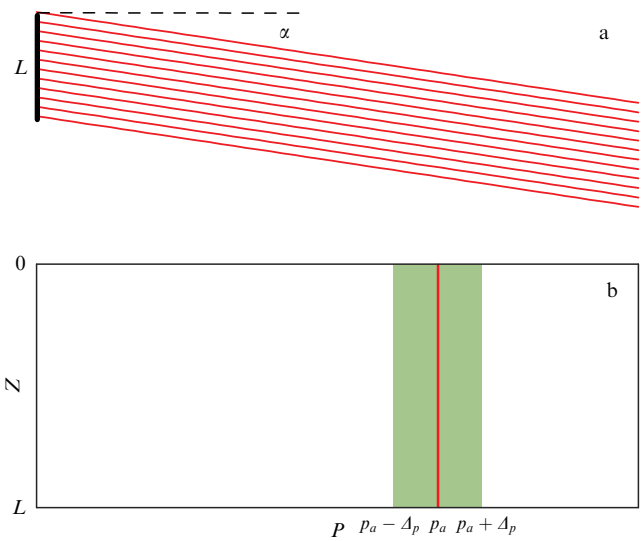

Figure 7. Antenna in a free space. (a) Beam of parallel rays incident on the antenna. (b) Segment of the ray line and the fuzzy segment (green color) which corresponds to the beam.

In the case of free space with a constant sound speed c_0, this procedure reduces to the standard beamforming. The field on an antenna at a large distance from the source is formed by a beam of parallel rays (Fig. 7a). The segment of the ray line which represents the beam is given by the segment $p = p_a$, where $p_a = \sin\alpha$, whereas the respective fuzzy segment is given by a rectangular domain bounded by inequalities $0 < Z < L$, $p_a - \Delta_p < P < p_a + \Delta_p$ (Fig. 7b). If $\Delta_z \gg \lambda$, the filter kernel computed by formula (10) can be approximately presented in the form

$$\Pi(z, z') \approx \exp\left[ikp_a(z - z')\right] \frac{\sin\left[\pi(z - z')/\Delta_z\right]}{\pi(z - z')} \,. \tag{11}$$

Spatial filtering with such a kernel isolates contributions from waves propagating at grazing angles from the interval $\alpha \pm \lambda/\Delta_z$. If Δ_z approaches L, the width of the angular interval reaches values of the order of λ/L.

To apply the procedure discussed here (in both homogeneous and inhomogeneous media), the antenna should be sufficiently long. According to (1), the function $Y_\mu(z)$ is localized in the interval with a width of about Δ_z centered at $z = Z$. For this reason, the amplitudes of coherent states a_μ can only be found for the phase plane points μ with coordinates Z inside the interval $z_1 + \Delta_z/2 < Z < z_2 - \Delta_z/2$. In numerical results presented below, the integration in (8) and (10) is carried out only over such μ. Since in the examples considered here the scale Δ_z is small compared to $L = z_2 - z_1$, this leads to only a slight reduction in the integration domain σ_n. Furthermore, it should be mentioned that, because the amplitude of $Y_\mu(z)$ rapidly decays outside the interval $Z \pm \Delta_z/2$, the procedure works satisfactorily even for Δ_z close to L.

Let us mention the following fundamental point. The inaccuracy in the mathematical model of environment — which is the lack of strong fluctuations in δc in our example — can be the reason why calculations of the fuzzy segment σ_n will result in the domain of phase plane σ_n', which does not even intersect with σ_n. Such an error, admittedly, would not allow the isolation of the required field component.

This difficulty can be overcome by expanding the domain σ_n' to a size which 'warrants' the inclusion of σ_n. This should be done based on a priori information about possible variability in parameters of the environment model. An analog of such an expansion is the broadening of an antenna beam in a free space through a reduction in the antenna length or the use of only a part of its aperture.

The procedure of isolating the component $u_n(z)$ discussed here assumes that the fuzzy segments σ_n (and also their expanded variants) that correspond to different beams do not overlap. In a waveguide, this condition is valid only on sufficiently short propagation paths. With an increase in distance, the ray line fills the region allowed for the rays more densely. In this process, the dimensionless distances that correspond to neighboring segments become shorter, the fuzzy segments begin to overlap, and eventually the contributions of individual beams can no longer be resolved. In free space, a similar situation takes place in detecting waves from two or more sources such that the angular distance between them is smaller than the antenna beam width. In Section 8, we shall see that for pulsed signals the possibilities of resolving the contributions from individual beams are essentially broader.

6. Contribution of a noise component

Together with the field $u(z)$ to be analyzed, the antenna usually receives ambient noise (in our example, this is some sea noise [17]). We denote by $\eta(z)$ the complex amplitude of noise on the same carrying frequency f as $u(z)$. We assume that $\eta(z)$ is a statistically homogeneous random function with a zero mean and the correlation function $Q(z-z') = \langle \eta(z)\eta^*(z')\rangle$.

To estimate the contribution of noise in the filter output signal given by relationships (9) and (10), we expand the noise field in coherent states

$$\eta(z) = \lambda^{-1}\int \mathrm{d}\mu\, b_\mu Y_\mu(z)\,, \quad b_\mu = \int \mathrm{d}z\, Y_\mu^*(z)\eta(z)\,.$$

As can be readily seen,

$$\left\langle |b_\mu|^2\right\rangle = \int \mathrm{d}z\,\mathrm{d}z'\, Y_\mu^*(z)\, Y_\mu(z')Q(z-z')\,. \tag{12}$$

The noise field is formed by waves propagating under the grazing angles from the interval $-\chi_{\max} < \chi < \chi_{\max}$. For simplicity, we assume that energy is uniformly distributed over angles. Then, one can take $l_\eta = \lambda/\chi_{\max}$ as an effective scale of the correlation function $Q(z)$. Assuming that $l_\eta \ll \Delta_z$, the noise correlation function on the right-hand side of (12) is written in the form

$$Q(z,z') = \left\langle |\eta|^2\right\rangle \frac{\lambda}{\chi_{\max}}\,\delta(z-z')\,.$$

Then, taking into account (5),

$$\left\langle |b_\mu|^2\right\rangle = \left\langle \eta^2\right\rangle \frac{\lambda}{\chi_{\max}}\,. \tag{13}$$

The noise component exiting the filter is

$$\eta_{\mathrm{s}}(z) = \lambda^{-1}\int_\sigma \mathrm{d}\mu\, b_\mu Y_\mu(z)\,, \tag{14}$$

where σ is the fuzzy segment which corresponds to the component of field $u(z)$ being isolated. Since $\eta_{\mathrm{s}}(z)$ is localized mainly within the interval of depths that correspond to the aperture of the antenna, and function b_μ is localized inside the fuzzy segment σ, from (4) one gets an approximate equality:

$$\int_0^L \mathrm{d}z\,\left|\eta_{\mathrm{s}}(z)\right|^2 \simeq \lambda^{-1}\int_\sigma \mathrm{d}\mu\,|b_\mu|^2\,. \tag{15}$$

Averaging this expression while taking into account (13) and assuming that $\langle|\eta_{\mathrm{s}}(z)|^2\rangle$ varies but weakly along the antenna aperture, we get

$$\left\langle |\eta_{\mathrm{s}}|^2\right\rangle = \left\langle |\eta|^2\right\rangle \frac{s_\sigma}{L\chi_{\max}}\,, \tag{16}$$

where s_σ is the area of σ.

For an antenna in free space, $s_\sigma = \lambda L/\Delta_z$ (see Fig. 7). Choosing the largest possible scale of coherent state $\Delta_z \simeq L$, we find

$$\frac{\left\langle |\eta_{\mathrm{s}}|^2\right\rangle}{\left\langle |\eta|^2\right\rangle} = \frac{\lambda}{L\chi_{\max}}\,.$$

This relationship allows a simple interpretation. From the total noise field formed by plane waves propagating at grazing angle χ lying in the interval with a width of the order of $\chi_{\max}$, the antenna beam 'admits' only waves with angle χ at the interval with the width of λ/L.

The main result of this section is expression (16), according to which the level of noisy signals at the filter exit is proportional to the area of fuzzy segment σ. For this reason, in order to reduce the level of noise, the scale Δ_z should be selected so as to minimize σ. However, in the preceding section, we have seen that, to 'overcome' the inaccuracy of the model, one may need an increase in σ. The incurred deterioration of the signal-to-noise ratio will be the payment for the possibility of reliably isolating the required field component.

7. Source localization

In this section, we consider an application of the procedure for isolating the ray beam contribution described in Section 5 to the problem of source localization, i.e., reconstruction of its coordinates based on acoustic measurement data.

A traditional method to solve this problem is based on using so-called matched field processing [12, 18, 19]. The *measured* field $u(z)$ at the aperture of a receiving antenna with length L is compared with the fields $U(z,\mathbf{R})$ on the same antenna *calculated* for test sources placed at different points in the waveguide $\mathbf{R}$. A quantitative characteristic of the resemblance between $u(z)$ and $U(z,\mathbf{R})$ is provided by the uncertainty function

$$C(\mathbf{R}) = \frac{\left|\int_0^L u(z)U^*(z,\mathbf{R})\,\mathrm{d}z\right|}{\left(\int_0^L \mathrm{d}z\,\left|u(z)\right|^2\right)^{1/2}\left(\int_0^L \mathrm{d}z\,\left|U(z,\mathbf{R})\right|^2\right)^{1/2}}\,. \tag{17}$$

An estimate for the source position $\mathbf{R}$ corresponds to the maximum of this function. In practice, the efficiency of this approach is limited by unavoidable inaccuracy in the environment model, which is manifested especially strongly under multipath propagation conditions.

To overcome problems related to limited information on the environment, a series of robust algorithms has been

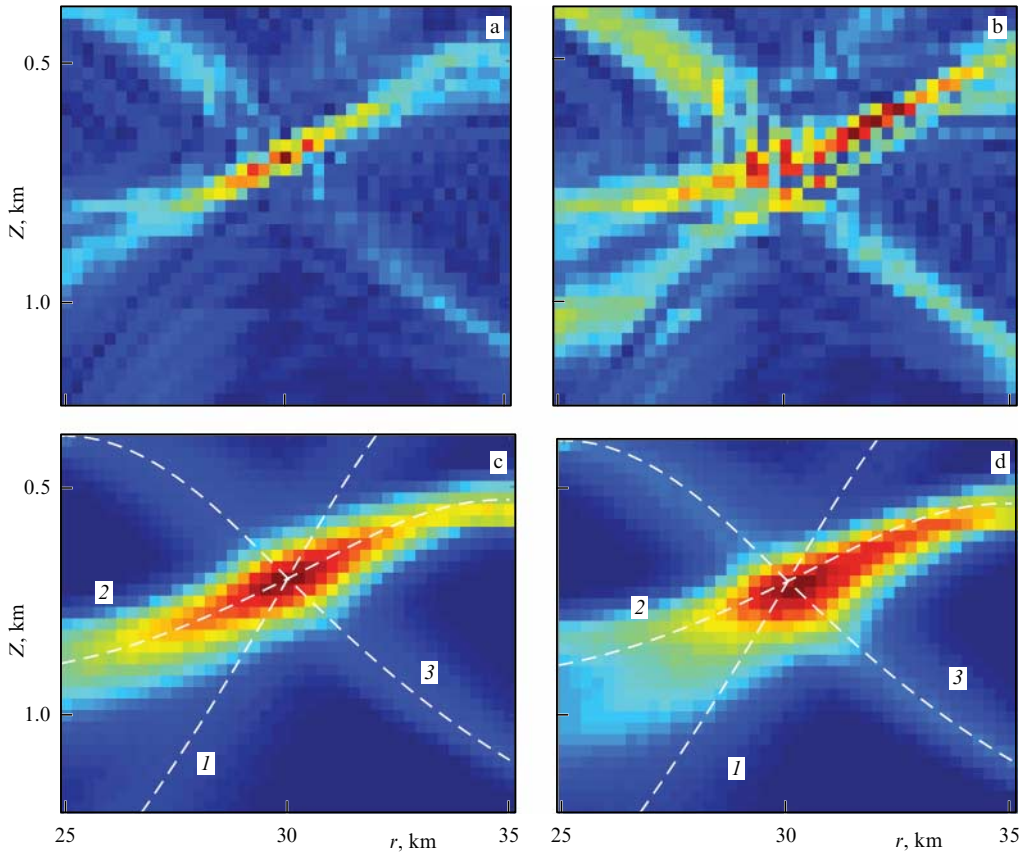

Figure 8. Uncertainty function $C(\mathbf{R})$ in unperturbed (a) and perturbed (b) waveguides. Uncertainty function $\tilde{C}(\mathbf{R})$ in unperturbed (c) and perturbed (d) waveguides. White dashed lines depict central rays of beams *1*, *2*, and *3* and their continuations for $r > r_s$. Each line is labelled with the number of the respective beam.

proposed. One of them is based on the method of spatial processing under multiple constraints [20]. In the framework of this method, the measured field is compared to the fields calculated for the source coordinates and some medium parameters lying in some admissible intervals [18, 21, 22]. In the framework of yet another known approach, in addition to the parameters sought for, one adds a set of parameters characterizing the propagation environment. The problem in this case consists in finding the entire set of unknown quantities based on Bayesian estimation theory [23, 24]. The description of this and other methods of matched signal processing is the subject of a vast literature (see monographs [12, 19] and review [25]). Nevertheless, the lack of information on the environment remains a serious problem [26], explaining the continuing studies on this topic.

As an alternative, we consider the following approach. For each test point $\mathbf{R}$, with the help of ray computations, we find all N ray beams that leave the point and arrive at the antenna, and for each beam we find the related fuzzy segment σ_n, $n = 1, \ldots, N$. Assuming that the source which creates the field $u(z)$ on the antenna is located at point $\mathbf{R}$, with the help of N filters (9), we isolate from $u(z)$ the components $u_n(z)$. The 'energy' of each isolated component $\int_0^L |u_n(z)|^2 \, \mathrm{d}z$ should be maximal for point $\mathbf{R} = (r_s, z_s)$, which corresponds to the true source position. For this reason, we take as the uncertainty function

$$\tilde{C}(\mathbf{R}) = \sum_{n=1}^{N} \int_0^L |u_n(z)|^2 \, \mathrm{d}z \left(\int_0^L |u(z)|^2 \, \mathrm{d}z \right)^{-1}. \qquad (18)$$

This is an example of so-called quadratic processing [25]: isolation of uncorrelated signals arriving from different directions and their noncoherent summation. If the fuzzy segments do not intersect, in analogy with (15),

$$\int_0^L |u_n(z)|^2 \, \mathrm{d}z \simeq \lambda^{-1} \int_{\sigma_n} |a_\mu|^2 \, \mathrm{d}\mu. \qquad (19)$$

In a homogeneous space, $N = 1$ and the value of $\tilde{C}(\mathbf{R})$ is proportional to the 'energy' of the antenna output signal with the main antenna beam oriented toward point $\mathbf{R}$.

It is natural to expect that the change from uncertainty function $C(\mathbf{R})$ to $\tilde{C}(\mathbf{R})$ reduces the demand to the accuracy of the environment model. Indeed, the use of $C(\mathbf{R})$ requires accurate computations of the complex amplitude of the total field at the antenna $U(z, \mathbf{R})$. In Section 4, it was explained that this is difficult to achieve in conditions of multipath propagation. On the other hand, in order to use the function $\tilde{C}(\mathbf{R})$, one in fact only needs to determine the fuzzy segments σ_n which, as we have seen, can be found with an unperturbed waveguide model, provided the perturbation δc is weak.

Figure 8 shows examples of uncertainty functions computed for the model of waveguide described in Section 2 in a situation when the antenna and the source to be localized are located as shown in Fig. 2. Figure 8a, c shows, respectively, the uncertainty functions $C(\mathbf{R})$ and $\tilde{C}(\mathbf{R})$ in the unperturbed waveguide ($\delta c = 0$). Such functions computed in the presence of one of the perturbation realizations are shown in Fig. 8b, d.

In Fig. 8a, we see that in an unperturbed waveguide, i.e., in the situation when the model of the medium is exact, the

function $C(\mathbf{R})$ has a sharp peak at the point of the true source location ($r_s = 30$ km and $z_s = 0.7$ km). This peak is so narrow that it is difficult to distinguish it in the figure. However, in the presence of a weak random perturbation (Fig. 8b), it 'breaks' into numerous local maxima.

In contrast, the function $\tilde{C}(\mathbf{R})$ in an unperturbed waveguide has a broad peak with the center at the point (r_s, z_s) (Fig. 8c). The transition from $C(\mathbf{R})$ to $\tilde{C}(\mathbf{R})$ in this case substantially reduces the accuracy of how the source coordinates are estimated. However, in the presence of perturbations, the function $\tilde{C}(\mathbf{R})$, different from $C(\mathbf{R})$, experiences almost no changes. It preserves a well pronounced peak with its center close to the point (r_s, z_s).

White dashed lines in Fig. 8c, d, intersecting at the point (r_s, z_s) depict central trajectories of beams *1*, *2*, and *3* from Fig. 2 and their continuations for $r > r_s$. The uncertainty function $\tilde{C}(\mathbf{R})$ is localized predominantly in the vicinity of these lines. This fact is explained as follows. Let us select the dashed line which corresponds to the nth beam. This beam partly overlaps with the beam formed by the rays emitted from an arbitrary point (r_s', z_s') of the line under consideration and reaching the antenna aperture. Hence, different fuzzy segments, which correspond to these two beams, partly overlap too. A filter tuned to the detection of signals from the point (r_s, z_s) will partly let in the signals from the point (r_s', z_s').

Thus, because of multipath propagation, the uncertainty function $\tilde{C}(\mathbf{R})$ in a waveguide has the form of several beams intersecting at the point where the source is located. In Fig. 8c, d, the dominant contribution comes from beam *2*, which, in fact, is focused close to the antenna. As mentioned in Section 2, its ray touches the caustic intersected by the antenna.

In a homogeneous space, where multipath propagation is absent, $\tilde{C}(\mathbf{R})$ is localized in the vicinity of the straight line that connects the source and the center of the antenna. In this case, the uncertainty function allows only the direction toward the source to be determined.

8. Pulsed signals

Here, we briefly consider the application of the procedure of Section 5 to isolate the contribution of a ray beam in the field emitted by a pulsed source. The complex amplitude of the field of such a source at a distance of observation $v(z, t)$ is synthesized from monochromatic fields $u(z, f)$ at frequencies f in the band of the emitted signal,

$$v(z,t) = \int \mathrm{d}f\, u(z,f) \exp(-2\pi \mathrm{i} f t)\,.$$

Since the ray trajectories in an underwater waveguide do not depend on frequency, the ray lines coincide for all f. However, from condition (7), it is clear that at least one of the coherent state scales Δ_z and Δ_p must depend on frequency.

The component of field $v(z, t)$, which represents the contribution of the nth beam, is synthesized from the components $u_n(z, f)$ found with the help of (8) or (9) for particular frequencies f. It is equal to

$$v_n(z,t) = \int \mathrm{d}f\, u_n(z,f) \exp(-2\pi \mathrm{i} f t)\,. \qquad (20)$$

In the transition from a tonal to a pulsed source, the possibilities of isolating the beam contributions become substantially wider: spatial resolution is augmented by the temporal one. Let us see this using a concrete example.

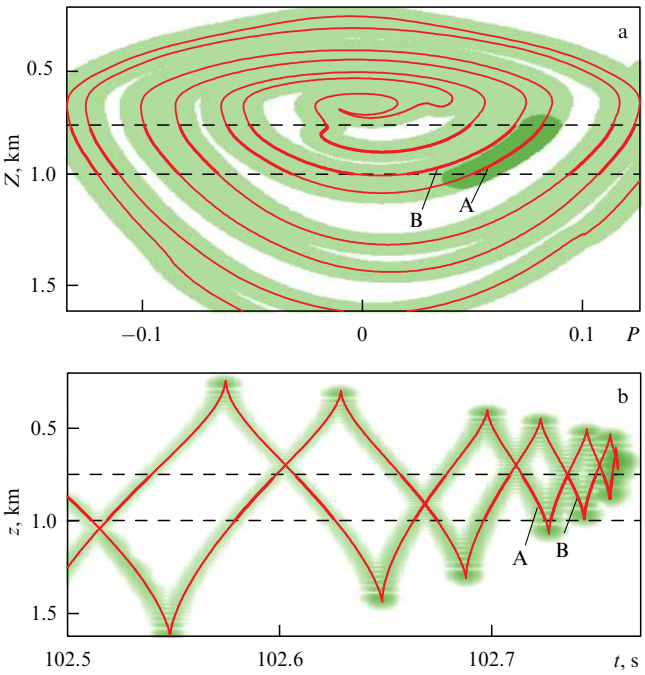

Figure 9. (a) Ray line (thin) and fuzzy ray line (shown in light green color) at a distance of 150 km from the source. (b) Distribution of intensity $|v(z,t)|^2$ in the plane time–depth and the timefront (thin line). Bold segments in panels (a) and (b) show arrivals of rays forming the beams, while dashed lines show horizons of antenna endpoints.

We continue to use the environment model described in Section 2 and assume that the receiving antenna covers the same depth range. Let a point source be at the same depth $z_s = 0.7$ km as in Fig. 2, but at a much larger distance from the antenna $r_s = 150$ km. We assume that the sound pulse $s(t) = \exp(-\pi t^2/\tau^2 - 2\pi \mathrm{i} f_0 t)$, where $f_0 = 500$ Hz and $\tau = 0.01$ s, is emitted. The emitted field is synthesized from monochromatic fields $u(z, f)$ at frequencies f lying in the range of 500 ± 150 Hz. The vertical coherent state scale Δ_z is taken to be 90 m at all frequencies.

The thin line in Fig. 9a depicts the ray line at a distance of 150 km from the source. A comparison with Fig. 3 shows that, in agreement with the remark at the end of Section 5, the ray line fills the region of the phase plane admissible to the rays more densely. The number of segments between the two dashed lines that show the depths of antenna endpoints increased from three in Fig. 3 to eleven in Fig. 9. Each segment presents a ray beam as earlier. The fuzzy ray line at the frequency of 500 Hz, which is localized close to the geometrical ray line in Fig. 3, nearly becomes a light-green spot in Fig. 9.

If at a distance of 30 km the fuzzy segments that correspond to separate beams do not overlap (see Fig. 3), this is not the case at a distance of 150 km. We denote as A and B two ray beams that correspond to two neighbor segments in Fig. 9a. The fuzzy segment that corresponds to beam A at frequency $f = 500$ Hz is shown in dark green color. It strongly overlaps with the fuzzy segment which corresponds to beam B (not shown in the figure), which implies that the contribution of beam A cannot be isolated from the total field in the case of a monochromatic source. This is true for all frequencies in the frequency band of the emitted signal.

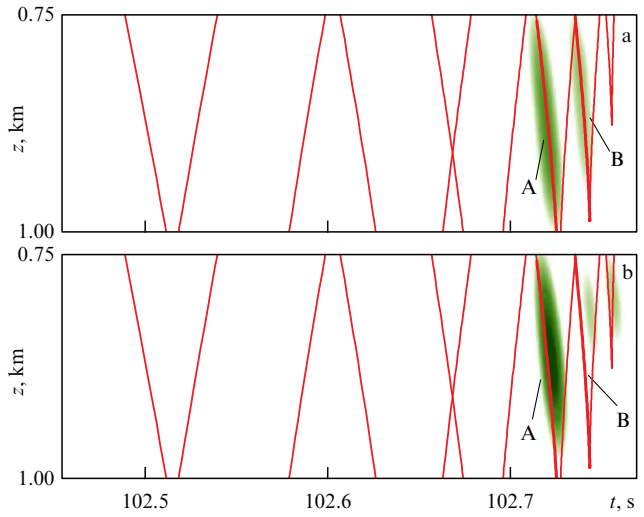

Figure 10. Distribution of intensity $|v_A(z,t)|^2$ in the time–depth plane in an unperturbed (a) and perturbed (b) waveguide. Thin lines show the segments of the timefront in the depth range covered by the antenna. Segments A and B are shown by bold lines.

Figure 9b displays the distribution of sound field intensity $|v(z,t)|^2$ at a distance of 150 km in the arrival time t–depth z plane. A thin solid line depicts the so-called timefront, each point of which shows the ray's arrival at the 150-km distance in the time–depth plane. The solid segments of the timefront show the arrivals of rays which form individual beams. The segments that correspond to beams A and B are labelled.

Figure 10 demonstrates the intensity distribution $|v_A(z,t)|^2$, where $v_A(z,t)$ is the result of isolating the contribution from beam A from the field $v(z,t)$ with the use of filtration at frequency f by formula (8) and subsequent synthesis by formula (20). Figures 10a and b show the distributions $|v_A(z,t)|^2$ in the unperturbed waveguide and in the presence of one of realizations of perturbation δc, respectively. Because of the intersection of fuzzy segments which correspond to beams A and B, when isolating the contribution of beam A at separate frequencies f, the filter also partially 'passes' the contribution from beam B. However, in Fig. 10, we see that the additional selection with respect to arrival time allows the contribution from beam A to be resolved. A similar situation takes place in free space by resolving signals arriving from close directions, but from sources placed at different distances from the antenna.

9. Conclusions

This study describes a processing method for signals detected by a receiving antenna in an inhomogeneous medium, which generalizes the standard beamforming procedure in a homogeneous space. From a formal viewpoint, the generalization is based on the change from the expansion of the field at the antenna in plane waves to the expansion in coherent states. The idea of the proposed approach is illustrated using an example of a two-dimensional acoustical waveguide in the deep sea. A two-dimensional model of a waveguide in the shallow sea can be considered analogously [27].

The proposed description can be easily generalized to a three-dimensional inhomogeneous acoustical medium, not necessarily a waveguide. In this case, in addition to z, one more transverse coordinate y is introduced, and the phase plane (P, Z) is generalized to the phase space (P_y, P_z, Y, Z). A coherent state will be represented by the product of two functions of the form (1): one will have arguments P_y, Y, and y, and the other one, P_z, Z, and z. In underwater acoustics, the use of a three-dimensional environment model will allow analyzing the work of a horizontal receiving antenna.

The proposed method needs a model of a propagation environment. It is used to calculate ray trajectories arriving at the antenna aperture. Based on these calculations, one finds the fuzzy segments which define the parameters of spatial filters isolating separate ray beams introduced in Section 5. It should be stressed that the presence of caustics does not create problems. Indeed, calculations deal with the parameters of trajectories in phase space where the singularities related to caustics are absent.

In the example considered, the plane-layered channel represents an idealized environment model. Its idealization lies in neglecting fluctuations in the speed of sound δc that are present in a real waveguide. For the applicability of our approach, the model should be accurate enough for calculations of fuzzy segments σ_n at the distance of observations. The results of simulations given in Section 4 indicate that, at a distance of 30 km, this requirement is fulfilled: the fuzzy segments computed for unperturbed and perturbed waveguides at least half-overlap. This allows beamforming in a fluctuating waveguide based on computations of trajectories for $\delta c = 0$. In the same section, it has been mentioned that model inaccuracy can be compensated by broadening the region σ_n.

The approach discussed in this paper can be applied for solving the same problems as matching field processing methods (isolation of a signal from a given direction, source localization, remote sounding, etc.). Its main advantage is the possibility of using an idealized environment model. The traditional methods are, as a rule, based on comparing measured and computed signals [25]. One cannot rely in this case on approximate calculations of trajectories. The need in calculations for a complex field amplitude at the antenna aperture significantly raises the requirements for the accuracy of the environment model, especially in conditions of multipath propagation.

In Section 7, using a concrete example, it was shown that the transition from the traditional method of solving localization problems based on matched field signal processing to our approach reduces the requirements for the environment model's accuracy. Close results were obtained in Refs [30, 31], where the isolation of ray beam contributions is also based on the field expansion in coherent states. However, these works use a simplifying assumption that the effect of perturbation δc is fully accounted for by multiplying the unperturbed component $u_n(z)$ by a random phase factor.

It should be noted that the estimate of limiting distances, for which our approach is applicable, requires additional studies. When detecting the field of a tonal source, the principal limitation is given by the condition that fuzzy segments which correspond to different beams not overlap. It holds only for relatively short paths. In Section 8, it was shown that in the case of a pulsed source this limitation becomes substantially weaker. It can be expected that our approach is applicable to work with pulsed sources, even under conditions when the effects of ray and wave chaos begin to appear [8, 28, 29]. However, this question is beyond the scope of the present paper and is not considered here.

This study was carried out in the framework of the state assignment of the Institute of Applied Physics RAS (project 0030-2021-0018). The author thanks his colleagues A Yu Kazarova and L Ya Lyubavin for their helpful discussions.

References

1. Van Trees H L *Detection, Estimation, and Modulation Theory* Pt. 4 *Optimum Array Processing* (New York: John Wiley and Sons, 2002)
2. Virovlyansky A L *J. Acoust. Soc. Am.* **141** 1180 (2017)
3. Virovlyansky A L, Kazarova A Yu, Lyubavin L Ya *IEEE J. Oceanic Eng.* **45** 1583 (2020)
4. Klauder J R, Sudarshan E C G *Fundamentals of Quantum Optics* (New York: W.A. Benjamin, 1968); Translated into Russian: *Osnovy Kvantovoi Optiki* (Moscow: Mir, 1970)
5. Schleich W P *Quantum Optics in Phase Space* (Berlin: Wiley-VCH, 2001)
6. Landau L D, Lifshitz E M *Mechanics* (Oxford: Pergamon Press, 1976); Translated from Russian: *Mekhanika* (Moscow: Nauka, 1973)
7. Goldstein H, Poole C, Safko J *Classical Mechanics* (San Francisco, CA: Addison Wesley, 2000)
8. Makarov D, Prants S, Virovlyansky A, Zaslavsky G *Ray and Wave Chaos in Ocean Acoustics*: *Chaos in Waveguides* (Ser. on Complexity, Nonlinearity and Chaos, Vol. 1) (Singapore: World Scientific, 2010)
9. Flatté S M (Ed.) et al. *Sound Transmission Through a Fluctuating Ocean* (Cambridge: Cambridge Univ. Press, 1979)
10. Colosi J A *Sound Propagation Through the Stochastic Ocean* (New York: Cambridge Univ. Press, 2016)
11. Virovlyansky A L, Makarova Iu M *Europhys. Lett.* **123** 54004 (2018)
12. Jensen F B et al. *Computational Ocean Acoustics* (New York: Springer, 2011)
13. Virovlyansky A L, Kazarova A Yu, Lyubavin L Ya *J. Acoust. Soc. Am.* **121** 2542 (2007)
14. Alonso M A, in *Phase-Space Optics*: *Fundamentals and Applications* (Eds M E Testorf, B M Hennelly, J Ojeda-Castañeda) (New York: McGraw-Hill, 2010) p. 237
15. Glauber R J *Quantum Theory of Optical Coherence. Selected Papers and Lectures* (Weinheim: Wiley-VCH, 2007)
16. Landau L D, Lifshitz E M *Quantum Mechanics*: *Non-Relativistic Theory* (Oxford: Pergamon Press, 1977); Translated from Russian: *Kvantovaya Mekhanika*: *Nerelyativistskaya Teoriya* (Moscow: Nauka, 1974)
17. Brekhovskikh L M, Lysanov Yu P *Fundamentals of Ocean Acoustics* (New York: Springer, 2003); Translated from Russian: *Teoreticheskie Osnovy Akustiki Okeana* (Moscow: Nauka, 2007)
18. Baggeroer A B, Kuperman W A, Mikhalevsky P N *IEEE J. Oceanic Eng.* **18** 401 (1993)
19. Etter P C *Underwater Acoustic Modeling and Simulation* (Boca Raton, FL: CRC Press, Taylor and Francis Group, 2018)
20. Schmidt H et al. *J. Acoust. Soc. Am.* **88** 1851 (1990)
21. Krolik J L *J. Acoust. Soc. Am.* **92** 1408 (1992)
22. Byun G et al. *J. Acoust. Soc. Am.* **147** 1231 (2020)
23. Richardson A M, Nolte L W *J. Acoust. Soc. Am.* **89** 2280 (1991)
24. Le Gall Y et al. *J. Acoust. Soc. Am.* **139** 993 (2016)
25. Sazontov A G, Malekhanov A I *Acoust. Phys.* **61** 213 (2015); *Akust. Zh.* **61** 233 (2015)
26. Baggeroer A B, in *Proc. of the 1st Intern. Conf. and Exhibition on Underwater Acoustics, Greece, Heraklion, 2013* (Eds J S Papadakis, L Bjørnø) p. 41
27. Virovlyansky A L *J. Acoust. Soc. Am.* **142** EL136 (2017)
28. Abdullaev S S, Zaslavskii G M *Sov. Phys. Usp.* **38** 645 (1991); *Usp. Fiz. Nauk* **161** (8) 1 (1991)
29. Virovlyansky A L, Makarov D V, Prants S V *Phys. Usp.* **55** 18 (2012); *Usp. Fiz. Nauk* **182** 19 (2012)
30. Virovlyansky A L *J. Acoust. Soc. Am.* **148** 2351 (2020)
31. Virovlyansky A L, Kazarova A Yu *Acoust. Phys.* **68** 162 (2022); *Akust. Zh.* **68** 190 (2022)